Molecular Biology of the Cell
Vol. 17, 2498–2512, June 2006

Specific and Nonspecific Membrane-binding Determinants Cooperate in Targeting Phosphatidylinositol Transfer Protein β-Isoform to the Mammalian *Trans*-Golgi Network[D] [V]

Scott E. Phillips,*† Kristina E. Ile,*† Malika Boukhelifa,* Richard P.H. Huijbregts,‡ and Vytas A. Bankaitis*

*Department of Cell and Developmental Biology, Lineberger Comprehensive Cancer Center, University of North Carolina School of Medicine, Chapel Hill, NC 27599-7090; and ‡Department of Biochemistry and Molecular Genetics, University of Alabama at Birmingham, Birmingham, AL 35294-0021

Submitted January 30, 2006; Revised February 13, 2006; Accepted March 6, 2006
Monitoring Editor: Reid Gilmore

Phosphatidylinositol transfer proteins (PITPs) regulate the interface between lipid metabolism and specific steps in membrane trafficking through the secretory pathway in eukaryotes. Herein, we describe the *cis*-acting information that controls PITPβ localization in mammalian cells. We demonstrate PITPβ localizes predominantly to the *trans*-Golgi network (TGN) and that this localization is independent of the phospholipid-bound state of PITPβ. Domain mapping analyses show the targeting information within PITPβ consists of three short C-terminal specificity elements and a nonspecific membrane-binding element defined by a small motif consisting of adjacent tryptophan residues (the $W_{202}W_{203}$ motif). Combination of the specificity elements with the $W_{202}W_{203}$ motif is necessary and sufficient to generate an efficient TGN-targeting module. Finally, we demonstrate that PITPβ association with the TGN is tolerant to a range of missense mutations at residue serine 262, we describe the TGN localization of a novel PITPβ isoform with a naturally occurring $S_{262}Q$ polymorphism, and we find no other genetic or pharmacological evidence to support the concept that PITPβ localization to the TGN is obligately regulated by conventional protein kinase C (PKC) or the Golgi-localized PKC isoforms δ or ε. These latter findings are at odds with a previous report that conventional PKC-mediated phosphorylation of residue Ser_{262} is required for PITPβ targeting to Golgi membranes.

INTRODUCTION

Because the discovery that a phosphatidylinositol transfer protein (PITP) plays an essential role in regulating the interface between lipid metabolism and membrane trafficking from the yeast *trans*-Golgi network (TGN; Bankaitis *et al.*, 1990; Cleves *et al.*, 1991a, 1991b), it has become increasingly clear that lipid metabolism regulates many individual trafficking steps throughout the secretory pathway (Cleves *et al.*, 1991a; DeCamilli *et al.*, 1996; Simonsen *et al.*, 2001). In vivo studies demonstrate PITPs either control the efficiency at which trafficking reactions occur (Bankaitis *et al.*, 1989, 1990; Cleves *et al.*, 1991b; Kearns *et al.*, 1997) or impart spatial organization to these reactions (Carmen-Lopez *et al.*, 1994; Nakase *et al.*, 2001; Vincent *et al.*, 2005). PITPs do so by coupling their ability to bind and/or transfer specific lipids to the coordination of lipid metabolic pathways with specific membrane trafficking steps (see Phillips *et al.*, 2006). In vitro reconstitution of various membrane trafficking or receptor-coupled signaling reactions also identify involvements for PITPs in these events (Hay and Martin, 1993; Ohashi *et al.*, 1995; Cunningham *et al.*, 1996; Jones *et al.*, 1998).

The available evidence indicates confident assignment of function for any individual PITP requires in vivo studies with model genetic systems. The reconstituted systems that show PITP dependence are remarkably promiscuous from the perspective of source of PITP. This is amply demonstrated by the stoichiometric interchangeability of yeast and mammalian PITPs in such reconstitutions (Ohashi *et al.*, 1995; Cunningham *et al.*, 1996; Jones *et al.*, 1998), even though these PITPs exhibit unrelated structural folds (Sha *et al.*, 1998; Yoder *et al.*, 2001; Tilley *et al.*, 2004). By contrast, in vivo studies show even very closely related PITPs play nonredundant functions in cells (Li *et al.*, 2000; Alb *et al.*, 2002, 2003; Routt and Bankaitis, 2004; Vincent *et al.*, 2005).

Mammalian cells express three soluble PITPs. PITPα and PITPβ share 77 and 95% primary sequence identity and similarity, respectively, and are encoded by distinct genes. The third, rdgBβ, is considerably more diverged and remains largely unstudied (Fullwood *et al.*, 1999). The shared homologies notwithstanding, PITPα and PITPβ are functionally distinct (Alb *et al.*, 2002, 2003). In this regard, PITPα binds PtdIns and PtdCho, whereas PITPβ binds both those phospholipids and, in addition, sphingomyelin (SM; De Vries *et al.*, 1995). Moreover, recombinant PITPα and PITPβ localize to distinct compartments, the former to the cytosol and nucleus and the latter to the cytosol and a perinuclear

This article was published online ahead of print in *MBC in Press* (http://www.molbiolcell.org/cgi/doi/10.1091/mbc.E06–01–0089) on March 15, 2006.

[D] [V] The online version of this article contains supplemental material at *MBC Online* (http://www.molbiolcell.org).

† These authors contributed equally to this work.

Address correspondence to: Vytas A. Bankaitis (vytas@med.unc.edu).

Abbreviations used: GFP, green fluorescent protein; MEF, murine embryonic fibroblast; PITP, phosphatidylinositol transfer protein; PtdCho, phosphatidylcholine; PtdIns, phosphatidylinositol; SM, sphingomyelin; TGN, *trans*-Golgi network.

compartment that is likely the Golgi complex (De Vries *et al.*, 1995, 1996; van Tiel *et al.*, 2002). The relationship between the distinct biochemical properties of these two PITP isoforms and localization and function (if any) remain to be determined.

Herein, we report that endogenous PITPβ (and a novel spliceoform thereof) localizes predominantly to TGN membranes and that localization is specified by a functionally redundant set of three short C-terminal motifs. These motifs are collectively insufficient to target a naive reporter to Golgi membranes, but cooperate with a $W_{202}W_{203}$ motif to generate an efficient TGN-targeting module. We also show that the phospholipid-bound status of PITPβ does not contribute to its association with the TGN. Finally, in contrast to a previous claim (van Tiel *et al.*, 2002), our data indicate that neither localization of PITPβ nor its novel spliceoform to Golgi membranes is obligately regulated by conventional protein kinase C (PKC)-mediated phosphorylation of residue serine 262.

MATERIALS AND METHODS

Mammalian Cell Culture and Transfections

Murine embryonic fibroblasts (MEFs) were derived from E16.5 wild-type and *PITPα*$^{-/-}$ embryos as previously described (Alb *et al.*, 2003). The mammalian cell lines used in this study were cultured in DMEM containing 10% fetal bovine serum, 1 U/ml penicillin G, 100 μg/ml streptomycin, and 4.2 μl β-mercaptoethanol (for 500 ml of complete medium). Cultures were incubated at 37°C and in 5% CO_2.

COS-7 cells were transfected using Lipofectamine Plus reagent (Invitrogen, Carlsbad, CA). Briefly, 24 h before transfection the cells were plated at 50–60% confluency in six-well plates containing glass coverslips. DNA (1.5–2 μg) was reconstituted in 100 μl of OptiMEM (Invitrogen), mixed with 2 μl of Plus reagent, and incubated at room temperature for 15 min. In a separate microcentrifuge tube, 3 μl of Lipofectamine was diluted in 100 μl of OptiMEM for each transfection. After 15 min, the solutions were mixed and then incubated for 15 min at 25°C. Cells were washed twice with OptiMEM and incubated at 37°C with DNA mixture in 1 ml OptiMEM for 3 h. Subsequently, 4 ml of complete medium was added, and cells were cultured for 18–24 h before processing for immunocytochemistry. MEFs were transfected using the Amaxa (Cologne, Germany) nucleofector following the manufacturer's directions.

Antibody Reagents

PITP antibodies used in this study included: a PITPβ isoform–specific rabbit polyclonal antibody directed against the C-terminal 25 amino acid of PITPβ (generous gift from Bruce Hamilton), a PITPα isoform–specific chicken polyclonal antibody directed against the last 15 amino acids of PITPα (Alb *et al.*, 2002), and the NT-PITP-antibody rabbit polyclonal immunoglobulin (Ig) raised against the N-terminus of PITPα and that recognizes both PITPα and PITPβ (generous gift of Prof. George Helmkamp, Jr.).

The following primary antibodies were used: a monoclonal antibody directed against actin (Chemicon, Temecula, CA), sheep polyclonal anti-TGN38 Ig (Serotec), monoclonal anti-GM130 antibodies (BD Bioscience, San Diego, CA), and murine monoclonal anti-giantin Ig (generous gift from Dr. Hans Peter Hauri, Switzerland). Secondary antibodies used included: Alexa fluorescein isothiocyanate 488 (Molecular Probes, Eugene, OR), Cy5-conjugated anti-mouse and fluorescein isothiocyanate–conjugated anti-mouse (Jackson ImmunoResearch, West Grove, PA), and goat anti-rabbit, goat anti-mouse, or goat anti-chicken horseradish peroxidase (HRP)-conjugated antibodies (Jackson ImmunoResearch).

Immunocytochemistry

Cells were cultured on glass coverslips. Cells were fixed for 15 min with 3.7% formaldehyde in phosphate-buffered saline (PBS), permeabilized in 0.2% Triton X-100 in PBS for 4 min, rinsed once in PBS, and then preincubated for 30 min in blocking buffer (2% BSA in PBS). Permeabilized cells were subsequently incubated with suitable primary antibody appropriately diluted in blocking buffer for 1 h at room temperature, rinsed four times 5 min with PBS, and then incubated with the secondary antibodies appropriately diluted in blocking buffer for 1 h. Cells were rinsed four times in PBS, and coverslips were mounted onto glass slides and examined in a Leica SP2 Laser Scanning Confocal Microscope (Leica, Deerfield, IL). Images were processed with the use of Adobe Photoshop 6.0 (Adobe Systems, Mountain View, CA).

In classifying PITP localization profiles as "'Golgi," two major criteria were applied. First, for to score a profile as Golgi the appropriate query profile (GFP or PITP) must exhibit obvious and predominant colocalization with a Golgi marker (TGN38 or GM130). Second, the Golgi component of the query profile must be the strongest signal recorded in the cell being scored. Failure to satisfy both these criteria resulted in a non-Golgi score. Fixed and stained samples were blinded before scoring to control for investigator bias.

Pharmacological Challenge

PITPα$^{-/-}$ MEFs were grown on glass coverslips to subconfluency and intoxicated with chelerethryne chloride (0.66 μM; Sigma, St. Louis, MO) or G109203X (10 nM; Sigma) for appropriate times. PKC activity in MEFs was also stimulated by exposure of cells grown on coverslips to PMA (100 nM, Sigma) for 15 min in serum-free medium. Cells were subsequently fixed for PITPβ immunostaining as described above. Cell-free extracts were prepared for parallel-treated cultures and processed for immunoblot analysis as described below.

SDS-PAGE and Immunoblotting

Cultures were rinsed with ice-cold PBS and scraped into lysis buffer (20 mM Tris-HCL, pH 7.4, 150 mM NaCl, 2 mM EDTA, 10 mM NaF, 1% Triton 1 mM orthovanadate supplemented with a cocktail of protease inhibitors (Complete; Roche, Indianapolis, IN). For preparation of cell-free extracts, cells (grown to confluency in a 100-mm dish) were incubated with 700 μl of lysis buffer at 4°C for 10 min and then scraped with a rubber policeman into microcentrifuge tubes. After centrifugation at 14,000 × *g* for 10 min, the supernatant was mixed in Laemmli sample buffer and heated for 5 min at 95°C. Samples were resolved by SDS-PAGE (10%) and transferred to nitrocellulose (Millipore, Billerica, MA). Membranes were blocked overnight at 4°C in TBST (5% dry nonfat milk in 0.05% Tween 20 in Tris-buffered saline) and then incubated for 3 h at room temperature with the appropriate primary antibodies diluted in TBST. Membranes were rinsed four times for 5 min each with TBST and then incubated with the appropriate HRP-conjugated secondary antibody for 1 h, and washed four times for 5 min each with TBST. Blots were developed on x-ray film (Eastman Kodak, Rochester, NY) using the enhanced chemiluminescence (ECL) Western blotting detection reagent (Amersham, Arlington Heights, IL).

Generation of PITPα-GFP and PITPβ-GFP cDNAs

PCR primers for rat-PITPα and rat-PITPβ cDNA sequences were flanked on the 5′ end with the restriction enzyme site HindIII and on the 3′ end with the restriction enzyme site BamHI. The HindIII-BamHI PCR fragments were cloned into the pEGFP-C1 plasmid (Clontech, Palo Alto, CA). Yeast plasmids harboring PITPα and PITPβ cDNAs (Skinner *et al.*, 1993) were used as templates in the PCR reactions used for generating the appropriate DNA fragments for cloning. The resulting plasmids were designated pRE772 (PITPβ-GFP) and pRE774 (PITPα-GFP). Primer sequences used are available from the authors by request.

Yeast Complementation Assay

Wild-type and mutant PITPβ or PITPβ-GFP cDNAs, as appropriate, were cloned into the multicopy yeast *URA3* vector YEplac195 such that the cDNA was expressed either under control of the powerful constitutive *PGK* promoter or the constitutively expressed but weaker *SEC14* promoter. This expression vector was transformed into the *sec14-1*^{ts} yeast strain (CTY 1-1A, MAT**a** *ura3-52 his3Δ200, lys2-810 sec14-1*^{ts}; Cleves *et al.*, 1991b) using the lithium acetate method of Ito *et al.* (1983). As matched controls, isogenic vectors with either no insert or with *SEC14* or *PITPβ* cDNA inserts were also transformed into the *sec14-1*^{ts} yeast host strain. Transformants were selected and cultured in uracil-free glucose minimal medium (Sherman *et al.*, 1983). Five OD_{600} equivalents of each strain were resuspended in 200 μl Tris-EDTA buffer and serially diluted 10-fold in Tris-EDTA buffer. An aliquot (5 μl) of each dilution was spotted on duplicate YPD agar plates. One plate was incubated at the 30°C (a permissive temperature for *sec14-1*^{ts} mutants) to report unrestrained growth and viability. The companion plate was incubated at 37°C (normally a restrictive temperature for *sec14-1*^{ts} mutants) to assess phenotypic rescue of *sec14-1*^{ts}.

Phospholipid-Transfer Assays

Assays were performed using cytosol prepared from the *sec14Δ cki1* host strain CTY303 expressing the desired PITP as described previously (Kearns *et al.*, 1998; Phillips *et al.*, 1999; Li *et al.*, 2000; Vincent *et al.*, 2005). Cytosol fractions generated from CTY303 variants expressing Sec14p (positive control) or no PITP (negative control) were generated and assayed in parallel with those fractions containing PITPα, PITPβ, or PITPβ variants.

Site-directed Mutagenesis

The QuickChange kit (Stratagene, La Jolla, CA) was used. Sequences of the various mutagenic primers used are available from the authors by request. All mutant versions generated were verified by nucleotide sequence analysis.

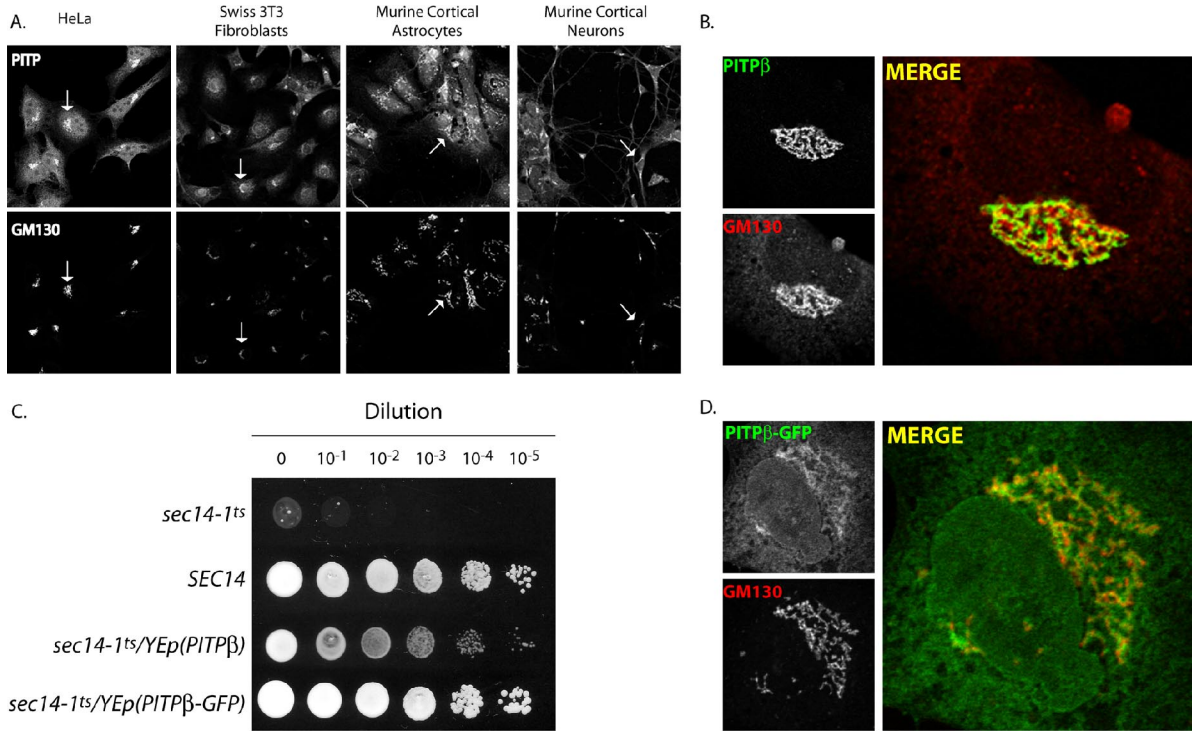

Figure 1. Endogenous PITP localization profiles. (A) Fixed and permeabilized cells of the indicated cell type were stained with a PITP antibody that detects PITPα and PITPβ and antibodies directed against the Golgi marker GM130. The PITP (top panels) and GM130 profiles (bottom panels) are shown. Arrows indicate one example of the clear colocalization of an endogenous PITP with Golgi membranes for each cell type and orient the remaining Golgi profiles in the matched panels. (B) PITP$\alpha^{-/-}$ MEFs were fixed and decorated with primary antibodies directed against PITP antigen or the *cis*-Golgi marker GM130. Representative individual profiles for endogenous PITPβ and GM130 are shown in the left panels, as indicated, and the merged profile is depicted in the right panel. (C) PITPβ-GFP chimera is a functional protein. Serial 10-fold dilutions of isogenic sets of a *sec14-1^{ts}* strain, derivatives of that strain carrying a high-copy plasmid (YEp) driving expression of either PITPβ, PITPβ-GFP, or a wild-type *SEC14* gene (as indicated) were spotted onto YPD agar and incubated at 37°C for 48 h. The 37°C condition, although permissive for growth of wild-type yeast, is restrictive for growth of *sec14-1^{ts}* yeast mutants. This *sec14-1^{ts}* growth defect is rescued by expression of either PITPβ or the PITPβ-GFP chimera, indicative of preservation of PITPβ activity in the PITPβ-GFP chimera. Strains used: CTY1-1A (*sec14-1^{ts}*), and CTY1-1A transformed with YEp(*SEC14*), YEp(*PITPβ*), and YEp(*PITPβ-GFP*), respectively. The respective PITPβ genes were driven by the strong and constitutively expressed yeast *PGK* promoter. (D) PITPβ-GFP faithfully targets to the Golgi complex. PITPα nullizygous MEFs were transfected with a PITPβ-GFP expression plasmid, fixed, and decorated with primary antibodies directed against GFP antigen and antibodies directed against GM130, as indicated. Representative individual profiles for PITPβ-GFP and GM130 are shown in the left panels, and the merged profile is depicted in the right panel.

RESULTS

Endogenous PITPβ Localizes to the Mammalian Golgi Complex

Previous experiments suggesting a Golgi localization of PITPβ in mammalian cells relied on microinjection of purified fluorophore-modified protein into cells (De Vries *et al.*, 1996) or creation of stable cell lines that overexpress PITPβ (van Tiel *et al.*, 2002). As a result, several key questions regarding PITPβ localization remain. First, it remains to be demonstrated whether endogenous PITPβ is genuinely a Golgi membrane–associated protein. Second, the precise distribution of PITPβ within the Golgi stack also remains to be determined.

Specific localization of endogenous PITPβ was complicated by our observation that antibodies generated against the extreme C-terminal 15- and 25-residue peptides of these proteins, although facile for distinguishing PITPα from PITPβ by immunoblotting, are not satisfactory for immunofluorescence experiments (unpublished data). To circumvent this issue, we used polyclonal antibodies raised against amino-terminal sequences conserved between PITPα and PITPβ. These antibodies (NT-PITP-antibody) are suitable for immunofluorescence but are not specific reagents in that these recognize both PITPα and PITPβ isoforms in immunoblotting experiments. The specificity issue notwithstanding, we inspected the endogenous PITP immunofluorescence staining profiles obtained with NT-PITP-antibody in an array of cell lines. Swiss 3T3 fibroblasts exhibited a strong perinuclear staining of what appears to be the Golgi apparatus and a diffuse signal in the cytoplasm and the nuclear matrix (Figure 1A). The PITP profiles obtained with Swiss 3T3 cells and NT-PITP-antibody as reporter were typical. Very similar results were also obtained with a variety of other cell lines including astrocytes, primary neurons, and COS-7, HeLa, and HEK293 cells. That the perinuclear PITP staining identifies the Golgi complex is indicated by the coincidence of this profile with that obtained for the *cis*-Golgi marker GM130 (Figure 1A). As the NT-PITP-antibody immunofluorescence profiles collected with immortalized cell lines represent the sum of endogenous PITPβ and PITPα distribution, and previous studies indicate PITPα localizes to the cytoplasm and nuclear matrix (De Vries *et al.*, 1996), these various localization profiles suggest that endogenous PITPβ targets to Golgi membranes in a variety of cell types.

To visualize endogenous PITPβ in isolation from PITPα, we used NT-PITP-antibody as PITP detector and took advantage of PITPα nullizygous primary cell lines that we had previously generated. The nullizygous MEFs are well suited for these experiments as these cells are phenotypically indistinguishable from wild-type MEFs and retain unadulterated levels of endogenous PITPβ (Alb *et al.*, 2002, 2003). As shown in Figure 1B, NT-PITP-antibody decorates an elaborate ribbonlike perinuclear structure in these PITPα$^{-/-}$ MEFs, and this structure is also stained by the *cis*-Golgi marker GM130. The GM130 and presumptive PITPβ staining profiles are very similar in form, but are not coincident. These data indicate that PITPβ does not localize to *cis*-Golgi membranes but, rather, localizes to a distinct subcompartment of the Golgi complex (see below). Very little staining of the cytoplasm or nucleus is observed, and staining of the lacelike ER is also evident. These staining profiles were absent when naive preimmune serum was substituted for NT-PITP-antibody in these experiments.

To confirm localization of the known PITPβ, we constructed a PITPβ-GFP chimera, where GFP was fused to the C-terminus of PITPβ. The activity of the PITPβ-GFP chimera was established with a yeast phenotypic rescue assay. This assay capitalizes on previous demonstrations that high-level expression of mammalian PITPs in yeast rescues the growth and secretory defects associated with inactivation of the essential yeast PITP Sec14p (Skinner *et al.*, 1993; Tanaka and Hosaka, 1994). This rescue is dependent on robust PtdIns-binding/transfer by the heterologous mammalian PITP (Alb *et al.*, 1995). As shown in Figure 1C, a *sec14-1^{ts}* yeast strain carrying an ectopic copy of the wild-type *SEC14* gene grows robustly at 37°C. By contrast, the isogenic *sec14-1^{ts}* strain fails to grow at all at 37°C, i.e., the restrictive temperature at which the thermolabile *sec14-1^{ts}* gene product is inactive. Expression of PITPβ-GFP restored robust growth to the *sec14-1^{ts}* yeast mutant at the restrictive 37°C temperature.

The functional PITPβ-GFP was expressed in MEFs and the distribution of the chimera was monitored. These localization experiments confirm an unambiguous affinity of PITPβ-GFP for Golgi membranes in MEFs (Figure 1D) and also in COS-7 cells (see below).

PITPβ Selectively Associates with the TGN

Although both Golgi and ER membranes harbor pools of PITPβ, Golgi localization predominates and how PITPβ targets to the Golgi membrane system is the focus of this study. To more precisely assign the Golgi subcompartment of residence for endogenous PITPβ, we performed a series of double-label immunofluorescence experiments. In these experiments, NT-PITP-antibody was used in combination with compatible antibodies raised against markers for specific Golgi compartments. These markers included GM130 for *cis*-Golgi, giantin for *cis*- and *medial*-Golgi, and TGN38 for the TGN. PITPα nullizygous MEFs were used to ensure specific detection of endogenous forms of PITPβ.

As shown in Figures 2, A and B, endogenous PITPβ exhibits little coincidence of staining with the *cis*-Golgi marker GM130, or the *medial*-Golgi marker giantin, even though the general profiles for PITPβ and these markers are very similar. Endogenous PITPβ species exhibit a higher degree of colocalization with the *trans*-Golgi membrane marker TGN38, however (Figure 2C). The predominant localization of PITPβ to TGN membranes is emphasized in a stereo reconstruction of the MEF Golgi apparatus generated from triple-label experiments monitoring PITP, giantin, and TGN38 (Supplemental Video, Figure S1). The rotating image distinguishes giantin staining from the yellow staining that reports colocalization of TGN38 and PITPβ. We infer from these experiments that PITPβ targets predominantly to the *trans*-aspect of the Golgi stack in MEFs.

During the course of these studies, we noted the existence in the NCBI Protein Database of an uncharacterized PITPβ spliceoform (referred to as PITPβ^{QGQR}, as opposed to canonical spliceoform that we refer to as PITPβ) that is invisible to our PITPβ-specific antibodies in immunoblot experiments (murine form, accession number AAH34676; rat form, AAH61538; human form, AAH31427). This spliceoform is detected by the NT-PITP-antibody, however, and the PITPβ localization profiles described in Figure 2 represent the sum of the PITPβ and PITPβ^{QGQR} profiles (these two spliceoforms are both expressed in MEFs; unpublished data). Defined GFP-chimeras permit localization of each spliceoform in isolation, however. As further described below, we show that both PITPβ-GFP and PITPβ^{QGQR}-GFP reporters target efficiently to similar (albeit not identical) Golgi subcompartments.

PITPβ C-terminal Motifs Necessary for TGN Targeting

The distinctive localization profiles for PITPβ and PITPα are remarkable in light of the high degree of primary sequence identity shared by these PITPs. To map the determinants specifying targeting of PITPβ to the mammalian TGN in an unbiased manner, we constructed a reciprocal series of PITPβ/PITPα hybrid proteins in the context of a functional PITP-GFP chimera. The functional status of key chimeras was confirmed in the heterologous yeast *sec14-1^{ts}* phenotypic rescue assay (Skinner *et al.*, 1993; described above and in Figure 1C). All chimeras generated were active in the yeast phenotypic rescue assay and were expressed both in PITPα$^{-/-}$ MEFs and in COS-7 cells. The respective intracellular distributions were imaged and quantified for both cell types. In describing the results of the mapping experiments, we present data obtained with MEFs and report the COS-7 data in Supplemental Materials.

The C-terminal 28 PITPβ residues are both necessary for PITPβ targeting to Golgi membranes and are sufficient to efficiently redirect PITPα to that location (Figure 3A). The results were robust because the incidence of Golgi targeting in cells was >90% for PITPβ and the PITPα/β chimera and <5% for PITPα and the PITP β/α chimera. Representative images for each chimera are shown in Figure 3B. In the imaging experiments reported herein, we typically identify the Golgi region by surveying the *cis*-Golgi marker GM130 but confirmed that assignment by costaining with the pan-Golgi marker wheat germ agglutinin and, for key reporter/mutant constructs, by costaining for TGN38 (see below).

Alignment of the PITPβ and PITPα C-terminal primary sequences identifies three motifs of greatest divergence between these isoforms. We refer to these motifs as BOX1, BOX2, and BOX3 (Figure 3C). Mutagenesis experiments, where each individual BOX region from PITPα was substituted for the corresponding BOX region of PITPβ, demonstrated that PITPβ^{KQE}, PITPβ^{QDPK}, and PITPβ^{MTD} all exhibited efficiencies of Golgi localization similar to those recorded for the PITPβ control (Figure 3, C and D). Thus, no single BOX motif is essential for PITPβ targeting to Golgi membranes. We also observed that swap of any two of the BOX domains from PITPα into the PITPβ context did not compromise association of PITPβ with TGN membranes (Figure 3, C and D). These data indicate that the presence of any single PITPβ motif is sufficient for maintenance of PITPβ localization to the Golgi complex. Parallel analyses of the localization properties of each chimera were also conducted

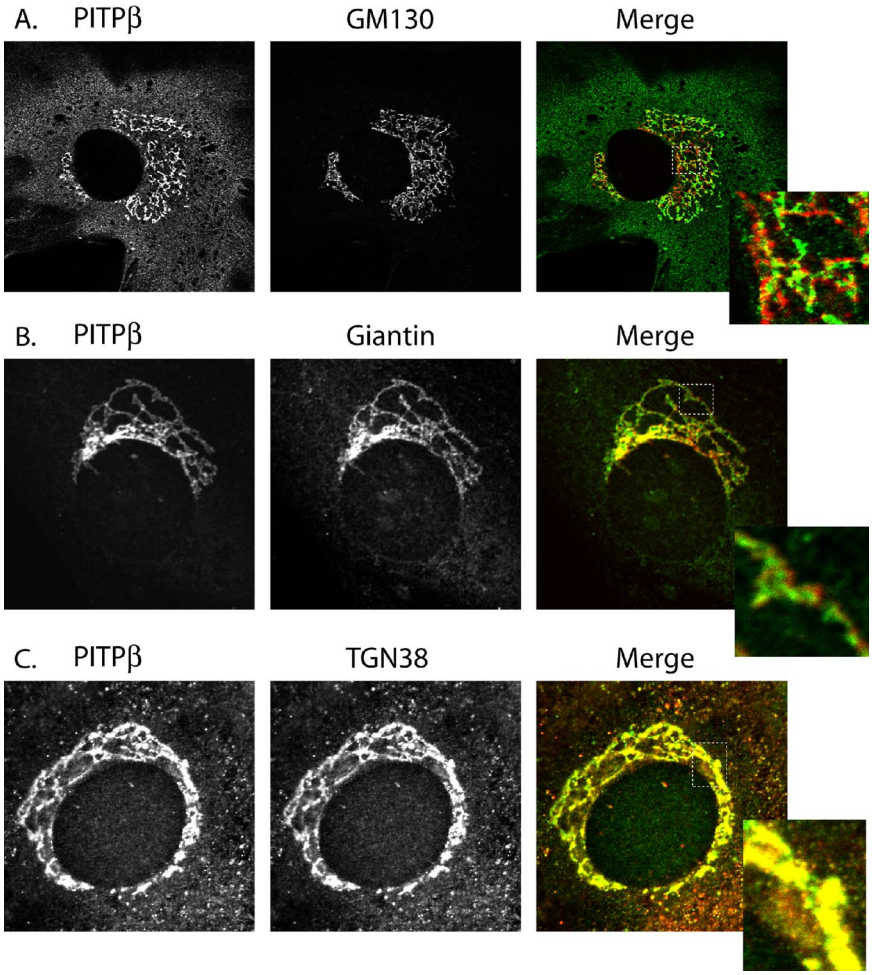

Figure 2. PITPβ localizes specifically to TGN membranes. PITPα nullizygous MEFs were fixed and decorated with primary antibodies directed against PITP antigen (rabbit polyclonal NT-PITP-antibody) and antibodies directed against either the *cis*-Golgi marker GM130 (A), the medial-Golgi marker giantin (B), or the *trans*-Golgi marker TGN38 (C). The individual and merged profiles are identified at the top. The respective insets represent a higher magnification of the boxed region of the corresponding merged profile for purposes of enhanced detail.

in COS-7 cells with essentially identical results (Supplemental Materials, Figure S2).

PITPβ C-terminal Motifs Sufficient for Targeting PITPα to Golgi Membranes

To address the dual criteria of necessity and sufficiency, we tested whether any BOX residues sufficient for PITPβ localization to the TGN were capable of redirecting PITPα to the same. To this end, PITPβ BOX1 or BOX3 residues were incorporated into the context of an otherwise wild-type PITPα. The localization profiles of both constructs (PITPα^{QET} and PITPα^{TSA}) fully recapitulated the nuclear and cytoplasmic distribution of the PITPα control (Figure 4A). Thus, neither BOX1 nor BOX3 has an assignable targeting function on its own in the context of PITPα. However, BOX2 residues, although dispensable for PITPβ targeting to the Golgi complex, increased the efficiency with which an otherwise wild-type PITPα reporter associates with Golgi membranes. That construct (PITPα^{KGSR}) was scored as targeting to Golgi membranes in 51% of the transfected cells analyzed. Although this level of targeting is not as robust as that observed with the PITPβ positive control (>90%), it is substantial when compared with the basal association of the PITPα control with the Golgi complex (ca. 5%; Figure 4A).

When multiple PITPβ BOX motifs were swapped into the PITPα context, an essentially complete redirection of a PITPα reporter to the TGN was observed. Combinatorial incorporation of PITPβ BOX1 and BOX2 residues, BOX1 and BOX3 residues, or BOX2 and BOX3 residues into the PITPα context yielded chimeras that efficiently targeted to Golgi membranes (Figures 4, A and B). For reasons detailed below, we were particularly interested in any role BOX2 or its individual residues may play in the localization of PITPβ to the TGN. In that regard, the dispensability of BOX2 residues for PITPβ Golgi targeting was further emphasized in a swap of BOX2 from PITPα for the PITPβ BOX2 in the context of a PITPα chimera that harbors the C-terminal 28 PITPβ residues. This PITP$\alpha^{QET\text{-}TSA}$ chimera is composed entirely of PITPα primary sequence, save 24 of 28 C-terminal residues where the PITPα BOX2 motif is substituted for that of PITPβ. Yet, PITP$\alpha^{QET\text{-}TSA}$ retains its capacity to target to Golgi membranes (Figures 4, A and B). Again, these conclusions were confirmed when these same chimeras were expressed in COS-7 cells and the corresponding localization profiles were scored (Supplemental Materials, Figure S3). The data indicate that the combination of any two of the PITPβ BOX motifs is sufficient to generate a robust Golgi localization signal in the context of PITPα.

PITPβ Ser_{262} Is Nonessential for Golgi Localization

The dispensability of BOX2 for PITPβ localization to TGN membranes was counter to the findings of van Tiel *et al.* (2002), who reported that phosphorylation of a BOX2 residue (S_{262}) is essential for PITPβ targeting to Golgi membranes. Yet, our demonstration that swap of PITPβ BOX2 residues significantly improved PITPα targeting to Golgi membranes (i.e., the

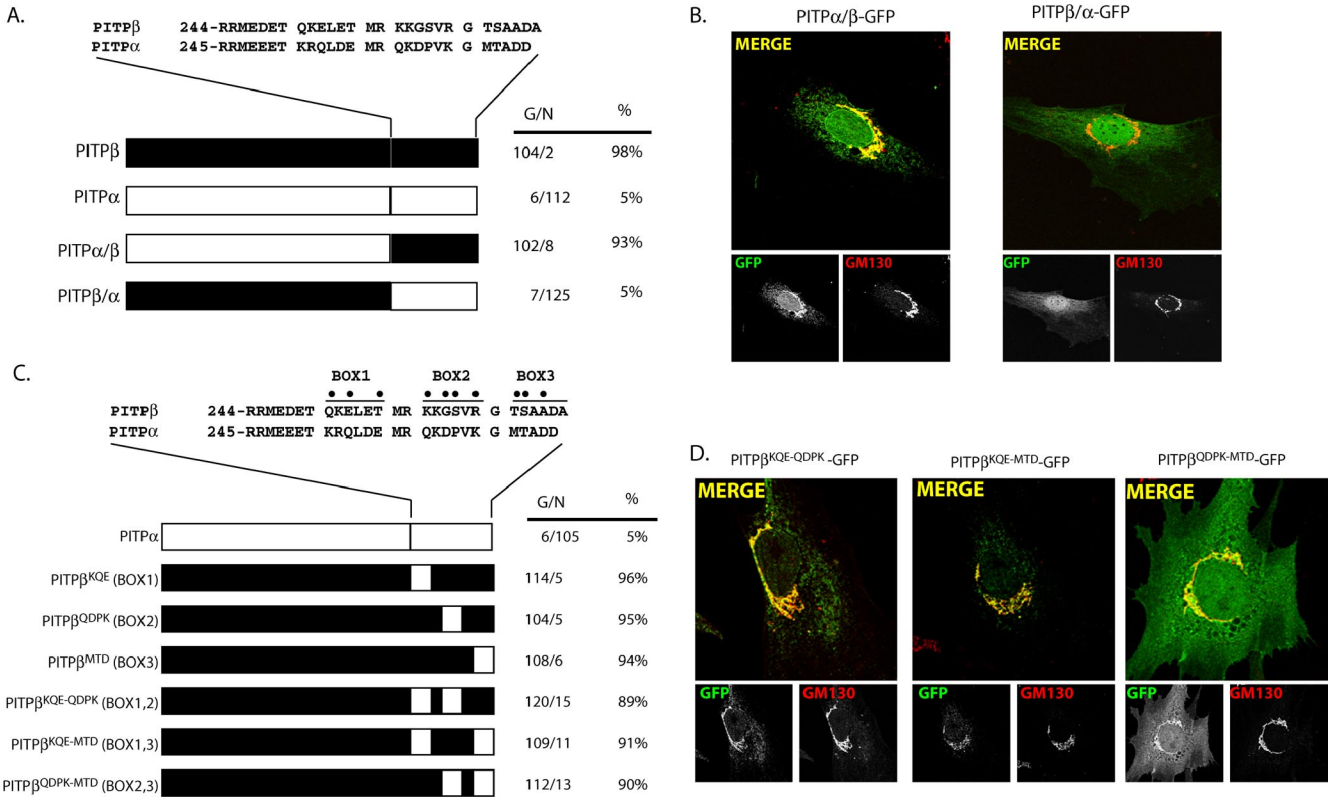

Figure 3. C-terminal PITPβ localization elements necessary for TGN association. (A) Alignment of the C-terminal 28 residues of PITPβ with the corresponding region of PITPα is given. Schematic illustrations of PITPα, PITPβ, and each of the reciprocal C-terminal swaps are depicted at bottom. At right, for each corresponding PITP version is given the number of imaged cells that exhibited a Golgi (G) or non-Golgi (N) immunofluorescence profile when that construct was expressed in MEFs as a PITP-GFP chimera and visualized along with the GM130 marker. The percentage of imaged cells with Golgi profiles is also given. (B) Imaging of PITPs with exchanged C-terminal regions. Representative localization profiles for PITPα/β-GFP and PITPβ/α-GFP when expressed in PITPα$^{-/-}$ MEFs are shown. Individual PITP-GFP and GM130 profiles are presented in the bottom panels underneath the corresponding merged profile. (C) Swap of divergent BOX motifs from PITPα into the context of PITPβ. The BOX motifs are defined at top, and the most divergent residues within each are highlighted (●). The series of hybrid PITPs analyzed is illustrated and each swap is further defined at left by identification of which PITPα residues were introduced to generate the swap. Quantification of PITPα$^{-/-}$ MEFs expressing each individual hybrid with respect to number of cells displaying Golgi (G) or non-Golgi (N) localization profile, along with percentages of cells displaying Golgi localization, is also given. (D) Representative images of PITPα$^{-/-}$ MEFs individually expressing each of the three PITPβ-GFP chimeras where two of the three BOX motifs were mutagenized to PITPα versions. The identities of the swaps are indicated at top. Individual PITP-GFP and GM130 profiles are presented in the bottom panels underneath the corresponding merged profile.

PITPα^{KGSR} construct; Figure 4A) is consistent with a more substantial role for BOX2 in Golgi targeting. To investigate these paradoxical findings in more detail, we analyzed the involvement of S_{262} itself in PITPβ localization. Consistent with the results of the BOX2 chimera experiments, PITPβ^{S262A}, PITPβ^{S262D}, PITPβ^{S262E}, and PITPβ^{S262P} all targeted to Golgi membranes as efficiently as the PITPβ control (Figure 4C). These results were recapitulated in the context of COS-7 cells (Supplemental Figures and Supplemental Table S1).

To determine whether an analogous phosphorylation may be sufficient to redirect PITPα to Golgi membranes, we incorporated phosphomimetic amino acids at the corresponding P_{263} residue of PITPα to generate the PITPα^{P263D} and PITPα^{P263E} mutants. The ability of each to associate with MEF TGN membranes was then assessed. Neither PITPα^{P263D} nor PITPα^{P263E} targeted to Golgi membranes any more efficiently than the PITPα control (Figure 4D). We repeated these analyses in COS-7 cells. Again, neither incorporation of the P_{263}S missense substitution, nor P_{263}E, into the context of PITPα-GFP had any major effect on the intracellular distribution of the chimera (Supplemental Materials, Supplemental Table S1).

A Novel PITPβ Isoform with Altered BOX2 Residues Targets to the TGN

All of the experiments described above rely on mutagenesis of canonical PITPβ. The novel murine PITPβ spliceoform described above (PITPβ^{QGQR}) differs from canonical PITPβ predominantly in BOX2 (Figure 4E). Interestingly, S_{262} of canonical PITPβ is Q_{262} in PITPβ^{QGQR}. PCR assays indicate both PITPβ and PITPβ^{QGQR} are expressed in PITPα$^{-/-}$ MEFs at approximately equal levels.

Localization experiments using GFP-tagged forms show PITPβ^{QGQR}, like PITPβ, associates with MEF Golgi membranes (Figure 4E). These results are consistent with data indicating S_{262} is nonessential for efficient targeting of PITPβ species to that compartment. PITPβ^{QGQR} displays a single nonconserved serine residue (S_{259}) in the region of divergence, but the S_{259}A mutation has no effect on targeting of a PITPβ^{QGQR}-GFP chimera to TGN membranes (Figure 4E). These data lead us to form two conclusions in addition to S_{262} dispensability for PITPβ targeting to Golgi. First, S_{259} does not offer an alternative phosphorylation site required for PITPβ^{QGQR} association with Golgi membranes. Second,

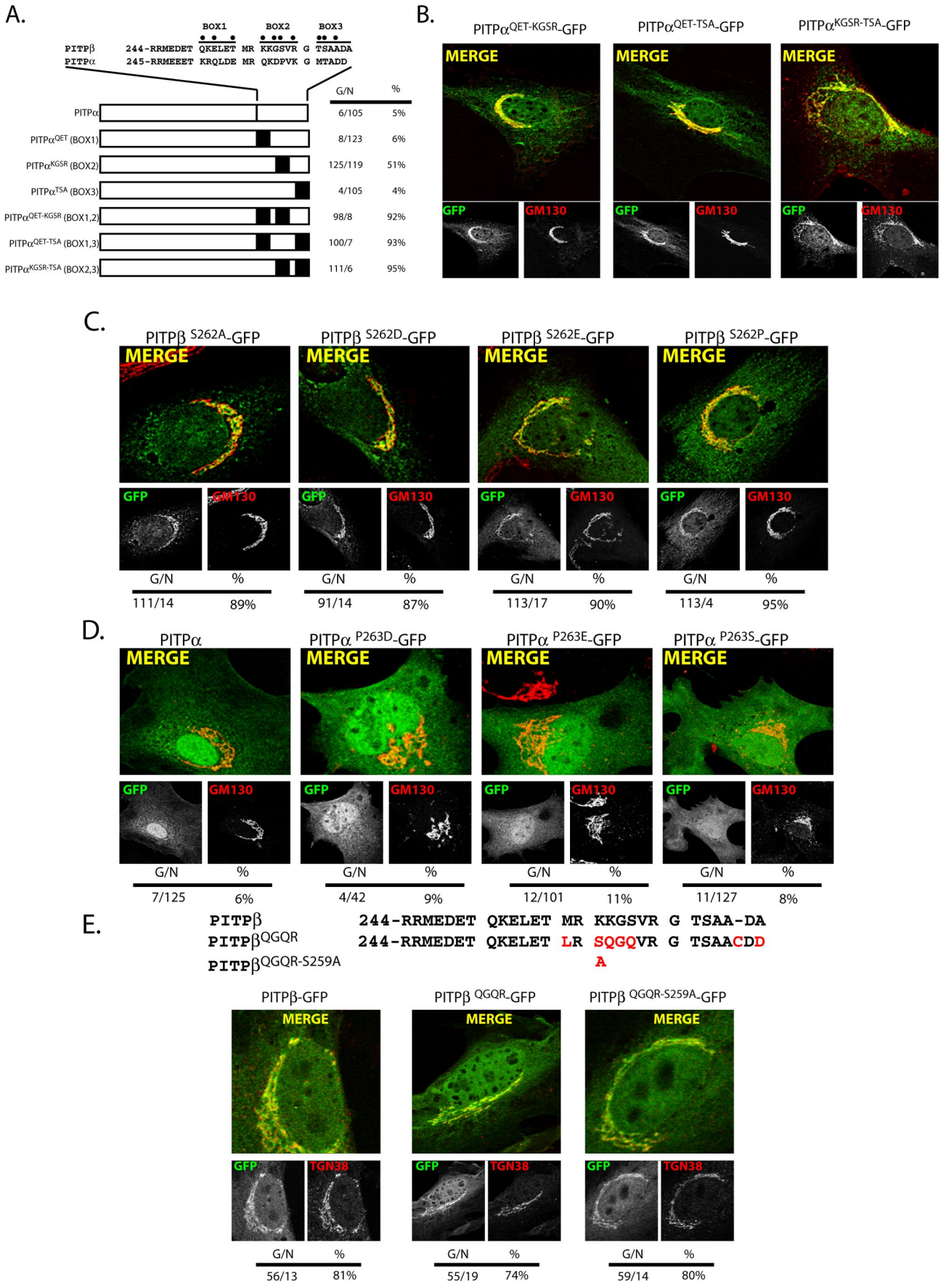
A.
BOX1
BOX2
BOX3
PITPβ 244-RRMEDET QKELET MR KKGSVR G TSAADA
PITPα 245-RRMEEET KRQLDE MR QKDPVK G MTADD
G/N
%
PITPα
6/105
5%
PITPα^QET (BOX1)
8/123
6%
PITPα^KGSR (BOX2)
125/119
51%
PITPα^TSA (BOX3)
4/105
4%
PITPα^QET-KGSR (BOX1,2)
98/8
92%
PITPα^QET-TSA (BOX1,3)
100/7
93%
PITPα^KGSR-TSA (BOX2,3)
111/6
95%
B.
PITPα^QET-KGSR-GFP
PITPα^QET-TSA-GFP
PITPα^KGSR-TSA-GFP
MERGE
GFP
GM130
C.
PITPβ S262A-GFP
PITPβ S262D-GFP
PITPβ S262E-GFP
PITPβ S262P-GFP
G/N
%
111/14
89%
91/14
87%
113/17
90%
113/4
95%
D.
PITPα
PITPα P263D-GFP
PITPα P263E-GFP
PITPα P263S-GFP
7/125
6%
4/42
9%
12/101
11%
11/127
8%
E.
PITPβ 244-RRMEDET QKELET MR KKGSVR G TSAA-DA
PITPβ^QGQR 244-RRMEDET QKELET LR SQGQVR G TSAACDD
PITPβ^QGQR-S259A A
PITPβ-GFP
PITPβ QGQR-GFP
PITPβ QGQR-S259A-GFP
TGN38
56/13
81%
55/19
74%
59/14
80%

Figure 4.

mammalian cells can express more than one PITPβ species in cells but, in this case, both PITPβ and PITPβ^{QGQR} isoforms home to Golgi membranes. Comparison of the localization profiles of PITPβ-GFP and PITPβ^{QGQR}-GFP chimeras indicates both target to the TGN, although PITPβ^{QGQR}-GFP also exhibits partial colocalization with the medial-Golgi marker mannosidase II (Supplemental Materials, Figure S4, A and B). PITPβ^{QGQR}-GFP also appears to target more efficiently to *cis*-Golgi membranes than does PITPβ-GFP (Supplemental Materials, Figure S4C). Thus, PITPβ^{QGQR} may represent more of a pan-Golgi PITPβ than the canonical PITPβ.

PITPβ Targeting to Golgi Membranes Is Independent of PtdIns- or SM-Transfer Activity

As described in detail below, the C-terminal 28 PITPβ residues are sufficient to redirect PITPα to Golgi membranes but are insufficient to target a naive protein to this intracellular location. These data suggest that multiple localization signals may be involved in localizing PITPβ to the TGN and that a subset of these determinants likely resides in the PITP domain itself. As PITP domains represent specific lipid-binding modules, PITPβ lipid-binding properties themselves could potentially define components of a combinatorial targeting signal.

To test this possibility, we took advantage of mutant PITPβ derivatives with selective defects in the loading/transfer of defined phospholipid substrates. Given that PITPβ is distinguished from PITPα in its ability to bind SM in addition to PtdIns and PtdCho, one attractive possibility is that SM loading contributes to the affinity of PITPβ for Golgi membranes. Data obtained from three independent lines of experimentation demonstrate that SM-loading and Golgi targeting are not strictly coupled. First, wholesale swap of the PITPα C-terminal 28 residues into the context of PITPβ leads to a PITP chimera that fails to associate with the Golgi complex (see Figure 3, A and B above). Yet, this PITPβ/α chimera exhibits robust SM transfer in vitro (Figure 5A). Second, reciprocal swap of the PITPβ C-terminal 28 residues into the context of PITPα results in a hybrid PITPα/β that efficiently targets to the Golgi complex (see Figure 3, A and B above). This PITPα/β chimera, while elaborating both PtdIns- and PtdCho- transfer activity, exhibits no detectable SM-loading/transfer activity in vitro (Figure 5A). Third, substitution of only two amino acids in PITPα to the cognate PITPβ residues is sufficient to confer robust SM-transfer activity to PITPα (PITPα^{LF221,225IL}; Figure 5A). Reciprocally, conversion of those cognate PITPβ residues to the corresponding PITPα residues strongly and specifically compromises the SM-transfer activity of PITPβ (PITPβ^{IL220,224LF}; Figure 5A). In neither case does modulation of SM-loading/transfer affect PtdIns- or PtdCh-transfer activity or PITP localization. PITPβ^{IL220,224LF} fully retains the ability to target efficiently to Golgi membranes, whereas PITPα^{LF221,225IL} does not (Figure 5B).

To probe the involvement of PtdIns loading in targeting of PITPβ to the TGN, we took advantage of mutants specifically defective in PtdIns-binding/transfer activity. PITPα residue T_{59} is essential for PtdIns-binding/transfer, but plays no role in PtdCho-binding/transfer (Alb *et al.*, 1995). The selective effects of the mutant translated to the PITPβ context as biochemical analyses confirmed that the corresponding PITPβ mutant (PITPβ^{T58D}) retains high levels of both PtdCho- and SM-transfer activity in the absence of measurable PtdIns-transfer activity (unpublished data). We constructed the PITPβ^{T58D}-GFP chimera and assessed its subcellular distribution in PITPα$^{-/-}$ MEFs. Imaging experiments show ca. 90% of the cells expressing PITPβ^{T58D}-GFP exhibited robust Golgi staining profiles, a score recapitulating that of the PITPβ control (Figure 5C). When the experiment was performed in COS-7 cells, PITPβ^{T58D}-GFP assumed an obvious Golgi localization in 91% of the 99 expressing cells imaged (90 Golgi/9 non-Golgi profiles). Thus, PtdIns-loading/transfer does not contribute to PITPβ targeting to Golgi membranes.

Uncoupling of Phospholipid-Transfer Activity from PITPβ Targeting to Golgi Membranes

Although neither PtdIns- or SM-loading/transfer activity are required for PITPβ association with the TGN, a combination of phospholipid-loading/transfer activities could contribute to such targeting. We therefore tested whether residue Ser_{165} is required for targeting of PITPβ to the Golgi complex. This residue lies in the PITP regulatory loop (Yoder *et al.*, 2001). The side-chain status of this residue is functionally important because incorporation of either alanine or glutamate at this position abolishes all PITPα phospholipid-transfer activities (van Tiel *et al.*, 2000).

The PITPβ^{S165A} mutant was generated and its biochemical properties were assayed in vitro. As reported by van Tiel *et al.* (2000) for PITPα^{S166A}, we too find PITPβ^{S165A} exhibited no measurable PtdIns-, PtdCho-, or SM-transfer activity, even though full-length PITPβ was readily detected in the cytosolic fractions by immunoblot (unpublished data). The S_{165}A missense substitution had no effect on PITPβ localization when assayed in PITPα$^{-/-}$ MEFs. PITPβ^{S165A}-GFP was targeted as efficiently to Golgi membranes as the PITPβ-GFP control (Figure 5D). Because PITPβ^{S165A} exhibits no detectable phospholipid-transfer activity, PITPβ^{S165A}-GFP association with Golgi membranes is independent of phospholipid-transfer activity.

We also expressed PITPβ^{S165,262A}-GFP in PITPα$^{-/-}$ MEFs and assessed the ability of this double mutant to target to TGN membranes. This experiment was motivated by the

Figure 4 (facing page). C-terminal PITPβ localization elements sufficient for redirecting PITPα to TGN membranes. (A) Swap of divergent BOX motifs from PITPβ into the context of PITPα. The BOX motifs are defined at the top, and the most divergent residues within each are highlighted (●). The series of hybrid PITPs is illustrated and each swap is further defined at left by identification of which PITPβ residues were introduced to generate the swap. Quantification of PITPα$^{-/-}$ MEFs expressing each individual hybrid with respect to number of cells displaying Golgi (G) or non-Golgi (N) localization profile, along with percentages of cells displaying Golgi localization, is also given. Representative images of PITPα$^{-/-}$ MEFs individually expressing: (B) each of the three PITPα-GFP chimeras where two of the three BOX motifs were mutagenized to PITPβ versions. The identities of the swaps are indicated at top. Individual PITP-GFP and GM130 profiles are presented in the bottom panels underneath the corresponding merged profile. (C) Each of the three PITPβ-GFP chimeras where residue S_{262} is mutagenized to A, D, E, or P as indicated. Individual PITPβ^{S262}-GFP and GM130 profiles are presented in the bottom panels underneath the corresponding merged profile. (D) Each of the three PITPα-GFP chimeras where residue P_{263} is mutagenized to S (the corresponding PITPβ residue) or the phosphomimetic residues D or E as indicated at top. Individual PITPα^{P263}-GFP and GM130 profiles are presented in the bottom panels underneath the corresponding merged profile. (E) The C-terminal 28 residues of PITPβ and the novel PITPβ^{QGQR} spliceoform are aligned at top, and the BOX motifs are identified. Differences in primary sequence are highlighted in red. The position of the S_{259}A mutation in PITPβ^{QGQR} is also indicated. Representative profiles for the corresponding GFP chimeras and GM130 are shown, as are the merged profiles. In B–E quantification of number of cells displaying Golgi (G) or non-Golgi (N) localization profile, along with percentages of cells displaying Golgi localization, is given.

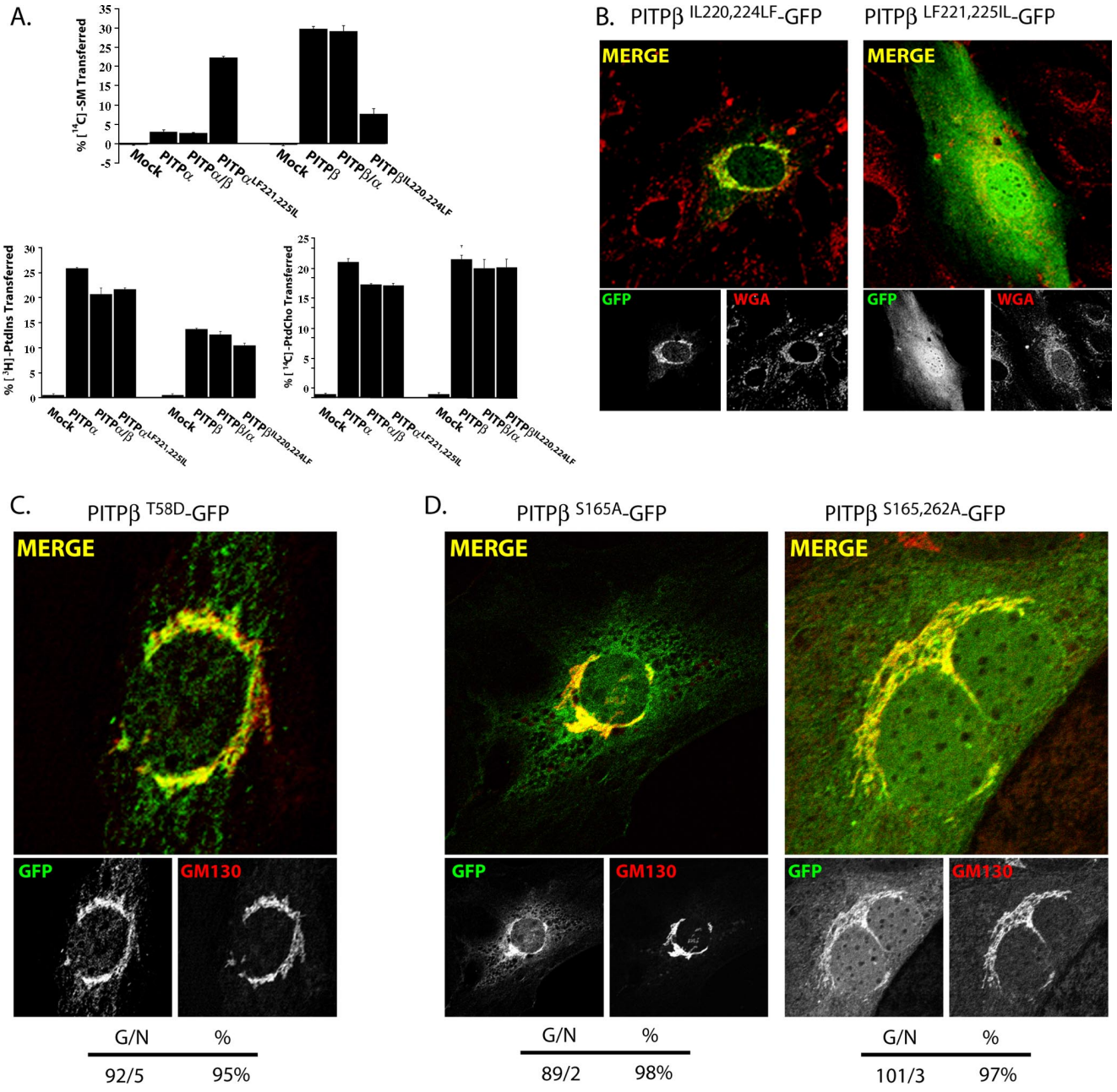

Figure 5. PITPβ localization to TGN membranes is independent of phospholipid loading. (A) Phospholipid-transfer properties of select PITP chimeras. Abilities of each individual PITP or PITP chimera to transfer [^{14}C]-SM, [^{3}H]PtdIns, or [^{14}C]PtdCho (as indicated) was determined in cytosol fractions prepared from yeast strain CTY303 (*sec14*Δ *cki1*Δ) expressing recombinant versions of the respective PITPs (Phillips *et al.*, 1999; Li *et al.*, 2000). CTY303/YEp(*URA3*) cytosol was prepared and used as negative control. Activity is represented as the percentage of total input radiolabeled phospholipid transferred from donor membranes to unlabeled acceptor membranes during the course of the experiment. Assay blanks represented addition of buffer alone to the transfer assay reactions, and these background values were subtracted from the other measurements. Values represent the averages of triplicate determinations from a representative experiment, and at least three independent experiments were performed. In the experiment shown, input phospholipid-transfer substrate was 19,850 cpm [^{14}C]SM; 21,050 cpm [^{3}H]PtdIns; 21,250 cpm [^{14}C]PtdCho. Background values for these respective transfer assays were 700, 315, and 820 cpm. A representative image of PITP$\alpha^{-/-}$ MEFs expressing a (B) PITP$\beta^{IL220,224LF}$-GFP or a PITP$\alpha^{LF221,225IL}$-GFP chimera. Cells were imaged for GFP and the pan-Golgi marker wheat germ agglutinin (WGA), as indicated. Corresponding merged profiles are shown. (C) PITPβ^{T58D}-GFP chimera. PITPβ^{T58D}-GFP and GM130 profiles are presented in the bottom panels underneath the corresponding merged profile. (D) PITPβ^{S165A}-GFP or a PITP$\beta^{S165,262A}$-GFP chimera. Cells were imaged for GFP and GM130, as indicated. Corresponding merged profiles are shown. For C and D, quantification of number of cells displaying Golgi (G) or non-Golgi (N) localization profiles, along with the percentages of cells displaying Golgi localization, are given for each construct at the bottom of the corresponding panel set.

demonstration that PITPα residue S_{166} and PITPβ residue S_{165} are minor PKC phosphorylation sites (van Tiel *et al.*, 2000, 2002). PITP$\beta^{S165,262A}$ is therefore devoid of the PKC phosphorylation sites for which there is any evidence of use. Yet, PITP$\beta^{S165,262A}$-GFP homes to TGN membranes in PITP$\alpha^{-/-}$ MEFs (Figure 5D). These data provide further

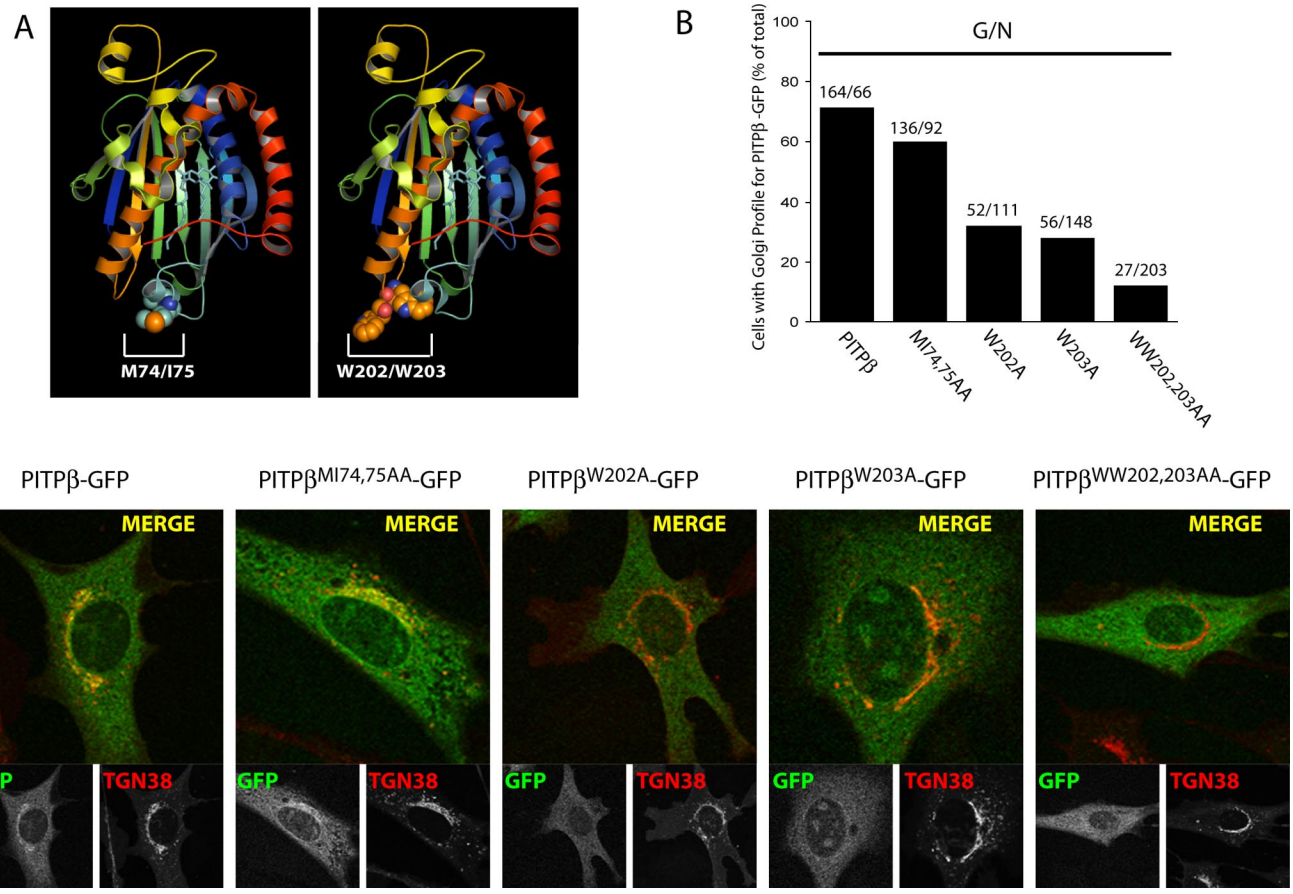

Figure 6. General PITP elements required for PITPβ localization to TGN membranes. (A) Ribbon diagram of the PtdIns-bound PITPα crystal structure with space-fill renditions of the $M_{74}I_{75}$ and $W_{202}W_{203}$ side-chains, as indicated. (B) Quantification of percentage of transfected PITPα$^{-/-}$ MEFs displaying Golgi localization profiles for each PITPβ-GFP construct (identified at bottom). The ratio of number of cells imaged with clear Golgi profiles (G) for the indicated PITPβ-GFP chimera to the number of cells imaged for that chimera that show a non-Golgi profile (N) is given above each corresponding bar. (C) Representative images of PITPα$^{-/-}$ MEFs expressing the indicated PITPβ-GFP chimeras. The localization profiles for the indicated PITPβ-GFP (bottom left panels), corresponding TGN38 (bottom right panels), and merged profiles (top panels) are presented.

support for our conclusion that PKC-mediated phosphorylation of PITPβ (at least on the presently known S_{165} and S_{262} sites) does not play an essential role in localization of this protein to mammalian TGN membranes.

A WW Motif Common to PITPα and PITPβ Contributes to Association of PITPβ with TGN Membranes

PITPα occupied with either PtdCho or PtdIns crystallizes as a dimer, and the dimerization interface is defined by two small hydrophobic motifs displayed on exposed loops of the PITP fold (Figure 6A; Yoder *et al.*, 2001; Tilley *et al.*, 2004). These two motifs are represented by $_{72}$FVRML$_{76}$ and $W_{203}W_{204}$ of PITPα and $_{71}$FVRMI$_{75}$ and $W_{202}W_{203}$ of PITPβ, respectively, and both are suggested to play critical roles in mediating membrane binding by PITPα (Schouten *et al.*, 2002; Tilley *et al.*, 2004). To test whether $_{71}$FVRMI$_{75}$ or $W_{202}W_{203}$ contribute to localization of PITPβ to the murine TGN, we mutagenized these motifs in the context of a PITPβ-GFP reporter and analyzed localization of the corresponding reporters in PITPα$^{-/-}$ MEFs. The comprehensive data are quantified in Figure 6B, and representative imaging profiles for the corresponding mutant PITPβ forms are given in Figure 6C.

Consistent with the view that the WW motif contributes to membrane binding, the PITPβ^{WW202,203AA}-GFP chimera failed to associate stably with PITPα$^{-/-}$ MEF TGN membranes. By contrast, PITPβ^{MI74,75AA}-GFP retained near wild-type efficiencies for TGN targeting (Figure 6, B and C). Although there is a consistent diminution in TGN association for the PITPβ^{MI74,75AA}-GFP chimera, the defect is minor. Essentially the same results were obtained with PITPβ^{F71A}-GFP and PITPβ^{VR72,73AA}-GFP chimeras. By contrast, the individual W_{202} and W_{203} residues each play important roles in localization of PITPβ, as evidenced by the obvious defects in PITPβ^{W202A}-GFP and PITPβ^{W203A}-GFP association with MEF TGN membranes (Figure 6B).

Previous data obtained from PtdIns loading assays performed with permeabilized cells indicated PITPα^{WW202,203AA} is strongly defective in PtdIns loading and is incompetent for the membrane interaction step of a phospholipid-transfer reaction (Tilley *et al.*, 2004). We obtained two lines of evidence that are not congruent with this conclusion, at least in the PITPβ context. First, biochemical assays for phospholipid-transfer activity demonstrate PITPβ^{MI74,75AA} and PITPβ^{WW202,203AA} exhibit significant levels of PtdIns-, PtdCho-, and SM-transfer activity in vitro (Figure 7A). Second, we again took advantage of the yeast phenotypic rescue assay described above to independently assess whether the phospholipid-binding/transfer activities of the double mu-

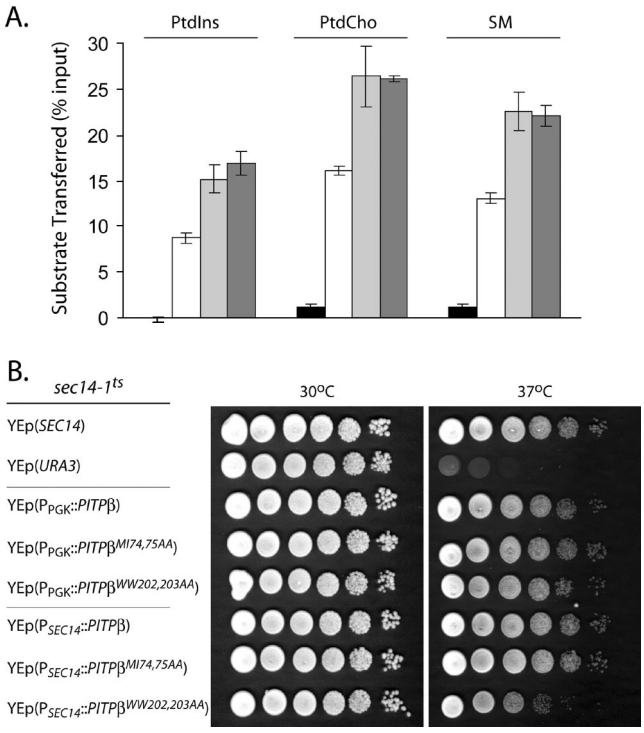

Figure 7. Properties of PITP$\beta^{W202W203}$ interaction with membranes. (A) Phospholipid-transfer assays. Abilities of each individual PITP to transfer [^{3}H]PtdIns, [^{14}C]PtdCho, or [^{14}C]-SM, (indicated at top) was determined in cytosol fractions prepared from yeast strain CTY303 (*sec14*Δ *cki1*Δ) expressing the negative control gene *URA3* (black bars), or recombinant versions of the respective PITPs (PITPβ, white bars; PITP$\beta^{MI74,75AA}$, hatched bars; PITP$\beta^{WW202,203AA}$, stippled bars). Activity is represented as the percentage of total input radiolabeled phospholipid transferred from donor membranes to unlabeled acceptor membranes during the course of the experiment. Values represent the averages of triplicate determinations from a representative experiment, and at least three independent experiments were performed. Assay blanks represented addition of buffer alone to the transfer assay reactions, and corresponding background values were subtracted from the other measurements. In this set of assays, input substrate was 14,792 cpm [^{3}H]PtdIns; 27,940 cpm [^{14}C]PtdCho; 22,216 cpm [^{14}C]SM, respectively. Background values were 295, 485, and 236 cpm for each respective assay. (B) PITP$\beta^{WW202,203AA}$ mutants preserve function as assayed in yeast. Serial 10-fold dilutions of isogenic sets of a *sec14-1^{ts}* strain, derivatives of that strain carrying a high-copy plasmid (YEp) driving expression of either PITPβ, PITPβ-^{WW202,203AA}, PITPβ-^{MI74,75AA}, or a wild-type *SEC14* gene (as indicated) were spotted onto YPD agar and incubated at 37°C for 48 h. Strains used were CTY1-1A (*sec14-1^{ts}*), and CTY1-1A transformed with YEp(*SEC14*), YEp(*PITP*β), YEp(PITPβ-^{MI74,75AA}), and YEp(*PITP*$\beta^{WW202,203AA}$), respectively. The PITPβ genes were driven by the strong and constitutively expressed yeast *PGK* promoter (P_{PGK}) or the weaker constitutively expressed *SEC14* promoter (P_{SEC14}), as indicated.

tant PITPs were strongly compromised. The results from that rescue assay also support the conclusion that both PITP$\beta^{MI74,75AA}$ and PITP$\beta^{WW202,203AA}$ are substantially functional proteins. As shown in Figure 7B, a wild-type yeast strain grows robustly at 30 and 37°C. By contrast, an isogenic *sec14-1^{ts}* strain grows only at the permissive temperature of 30°C and not at all at the restrictive temperature of 37°C, i.e., the temperature at which the thermolabile *sec14-1^{ts}* gene product is inactive. PITPβ expression from either a strong constitutive promoter (P_{PGK}) or a weaker constitutive promoter (P_{SEC14}) restored essentially wild-type growth properties to the *sec14-1^{ts}* yeast mutant. Similarly,

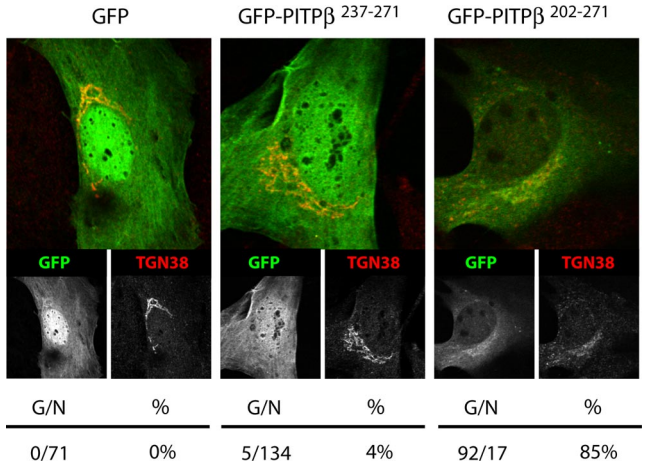

Figure 8. $W_{202}W_{203}$ and C-terminal BOX motifs in TGN targeting. Representative profiles for a GFP control, the GFP-PITP$\beta^{237–271}$ chimera, and the GFP-PITP$\beta^{201–271}$ chimera are shown. Quantification of transfected PITP$\alpha^{-/-}$ MEFs displaying Golgi localization profiles for each GFP-PITPβ construct is given at bottom as the ratio of number of cells imaged with clear Golgi profiles for the indicated GFP-PITPβ chimera to the total number of cells imaged for that chimera.

expression of either PITP$\beta^{MI74,75AA}$ or PITP$\beta^{WW202,203AA}$ from the P_{PGK} driver also supported efficient rescue of *sec14-1^{ts}*-associated growth defects at 37°C (Figure 7B). Rescue mediated by both mutant PITPβ forms was also recorded when the mutant proteins were expressed from the weaker P_{SEC14} promoter, although quality of rescue was diminished slightly under those conditions for PITP$\beta^{WW202,203AA}$ (Figure 7B).

Taken together, the data indicate neither PITP$\beta^{MI74,75AA}$ nor PITP$\beta^{WW202,203AA}$ exhibit dramatic defects in phospholipid-transfer activity and phospholipid loading. Because these various double mutant PITPs retain phospholipid-transfer activity, the PITP fold must remain unperturbed in the double mutants. We conclude that the TGN localization defects associated with mutation of $W_{202}W_{203}$ cannot be simply ascribed to a wholesale inability of PITPβ to interact with membranes.

PITPβ Motifs Sufficient for Redirection of GFP to the TGN

The collective data suggest it is the combination of weak membrane targeting/association signals defined by the C-terminal BOX residues and the $W_{202}W_{203}$ motif that specifies PITPβ association with TGN membranes. To test this prediction we fused the C-terminal 35 and 71 residues of PITPβ to the GFP C-terminus. The former chimera (GFP-PITP$\beta^{237–271}$) elaborates all three of the C-terminal BOX motifs, is predicted to preserve the C-terminal PITPβ helix, but lacks both the $W_{202}W_{203}$ motif and obviously lacks an intact PITP fold. The latter chimera (GFP-PITP$\beta^{201–271}$) elaborates both $W_{202}W_{203}$ and the three BOX motifs, is predicted to maintain the ultimate two PITPβ helices, but lacks an intact PITP fold. The chimeras were expressed in PITP$\alpha^{-/-}$ MEFs and their respective intracellular distributions were determined.

As expected, the GFP control distributes to the cytoplasm and nuclear matrix and fails to associate with Golgi membranes as evidenced by its lack of colocalization with the TGN marker TGN38 (Figure 8). This profile was recapitulated for the GFP-PITP$\beta^{237–271}$ chimera that harbors all three of the C-terminal BOX motifs but no $W_{202}W_{203}$ motif. By

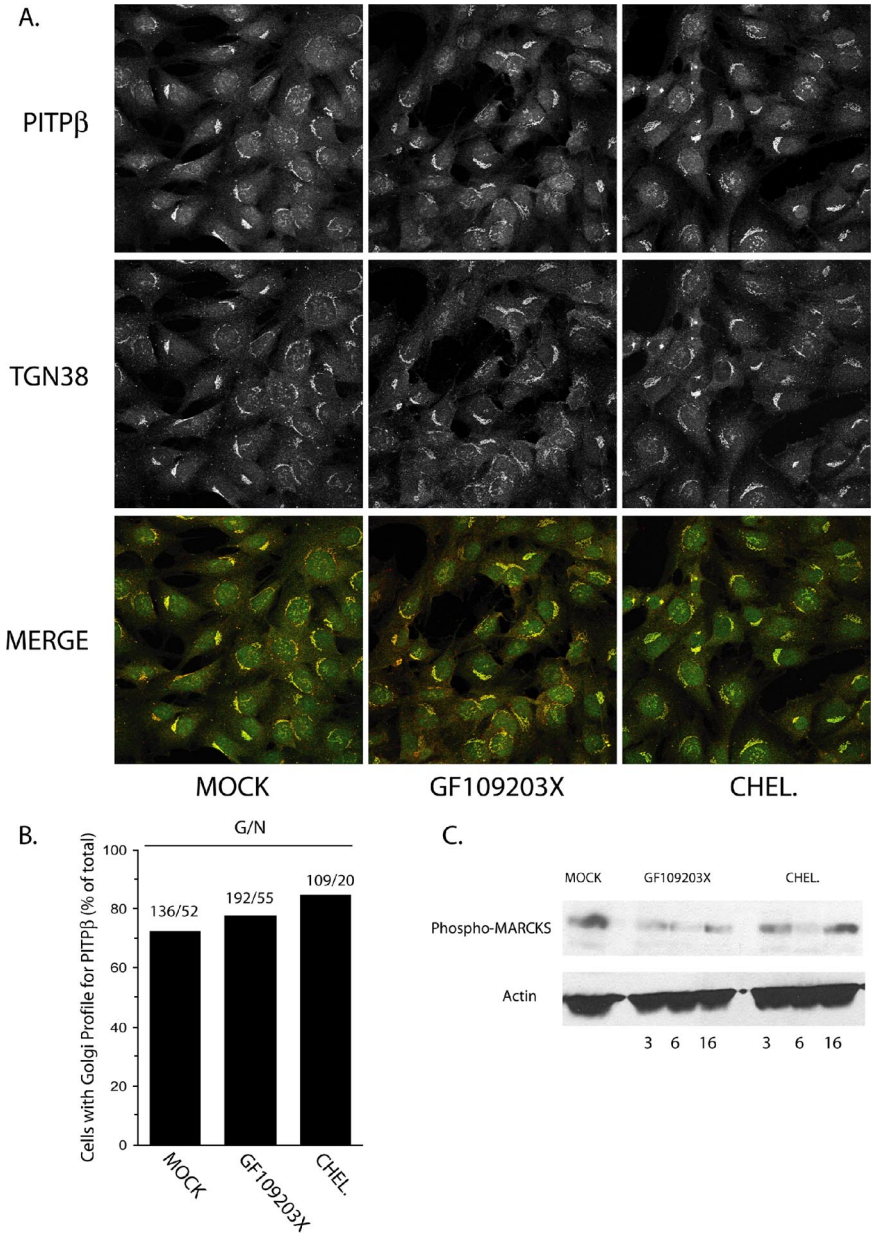

Figure 9. PITPβ localization and protein kinases C. (A) Profiles (individual and merged) for endogenous PITPβ and TGN38 in PITP$\alpha^{-/-}$ MEFs challenged with no inhibitor (MOCK), GF109203X (10 nM), or chelerythrine chloride (CHEL., 660 nM). The profiles shown at 6 h after challenge but are representative for what was observed at 3 and 16 h postchallenge as well. (B) Quantification of the imaging data presented in A. Number of cells imaged with clear Golgi profiles as a function of total number of cells imaged for each condition are indicated above each corresponding bar. (C) PITP$\alpha^{-/-}$ MEFs were challenged with no inhibitor (MOCK) or GF109203X (10 nM) or chelerythrine chloride (CHEL., 660 nM) for the indicated times. Cell-free lysates were prepared, resolved by SDS-PAGE and blotted to nitrocellulose, and blots were decorated with antibodies specific for phospho-MARCKs (a PKC substrate) and actin (loading control). Antibodies used detect MARCKS phosphorylated at $Ser_{159}Ser_{163}$ (Santa Cruz).

contrast, GFP-PITP$\beta^{201–271}$ targeted efficiently to PITP$\alpha^{-/-}$ MEF TGN as demonstrated by its colocalization with TGN38-positive structures (Figure 8). Some 85% of the cells showed coincident localization of GFP-PITP$\beta^{201–271}$ with the TGN. Thus, linking the PITPβ $W_{202}W_{203}$ motif with the three BOX motifs generated a targeting module that satisfies the dual criteria of necessity and sufficiency for specific association with TGN membranes.

PITPβ Association with TGN Membranes and Action of PKCs

The evidence reported herein is incongruent with the claim that PITPβ association with the Golgi complex depends on conventional PKC-mediated phosphorylation of S_{262} (van Tiel *et al.*, 2002). We therefore investigated what effect inactivation of conventional PKCs has on localization of PITPβ to the TGN. As a first approach, we applied a blunt pharmacological strategy. PITP$\alpha^{-/-}$ MEFs were intoxicated with two different inhibitors of conventional PKCs, and PITPβ distribution of was monitored at various times postchallenge. Neither GF109203X nor chelerythrine chloride intoxication had any effect, at any time, on the association of PITPβ with the MEF TGN (Figures 9, A and B). The efficacy of pharmacological challenge in inhibiting PKC activity was confirmed by monitoring phospho-MARCKS upon inhibitor challenge (Figure 9C).

In the pharmacological challenge experiments we used the NT-PITP-antibody as reporter. Thus, we were unable to distinguish between PITPβ and PITPβ^{QGQR} in those experiments. We therefore repeated these experiments using a PITP-GFP reporter and arrived at the same conclusions. PITPβ-GFP localization to the MEF TGN was resistant to challenge with GF109203X or chelerythrine chloride under the same conditions described in Figure 9C. Some 72% of mock-challenged MEFs exhibited a TGN profile for PITPβ-GFP (136/188 cells), and similar results were obtained upon

MEF intoxication with GF109203X (78%; 192/247 cells) or chelerythrine chloride (85%; 109/129 cells).

In a second approach, we derived MEFs from embryos individually nullizygous for either the nonconventional PKCδ or PKCε isoforms. Both of these isoforms localize to the mammalian Golgi complex (Lehel *et al.*, 1995; Storz *et al.*, 2004) and therefore represent reasonable candidate PKCs for which PITPβ is a physiological substrate. Again, localization to the murine Golgi of endogenous PITPβ species was unimpressed by genetic ablation of the PKCε or the PKCδ isoform (see Supplemental Materials, Figure S5A). Although we concur with van Tiel *et al.* (2002) that PITPβ can be phosphorylated by PKCs in vivo (i.e., PMA stimulates phosphorylation of endogenous PITPβ), we believe this effect is likely mediated through PKCδ because PMA challenge has no obvious effect on PITPβ phosphorylation status in PKCδ$^{-/-}$ MEFs (see Supplemental Materials, Figure S5B). Given that the Golgi-associated PKCδ plays no obligate role in targeting PITPβ to the TGN, we suggest PMA-stimulated phosphorylation of PITPβ reflects elevated PKCδ activity evoking an adventitious phosphorylation of vicinal proteins on Golgi membranes.

DISCUSSION

Herein, we identify endogenous PITPβ as a peripheral protein of mammalian TGN (and ER) membranes and describe a mechanism for PITPβ localization to those membranes. This mechanism involves four elements that define two distinct categories of targeting information. The first consists of three functionally redundant motifs that reside in the PITPβ C-terminal 28 residues. The second is represented by a $W_{202}W_{203}$ motif required for PITPβ association with TGN membranes. We posit these two sets of elements cooperate to localize PITPβ to the mammalian TGN. The cooperative contribution of both sets of elements generates a modular targeting code both necessary and sufficient for specific homing of proteins to the TGN.

How is specificity of targeting determined? The three motifs embedded in the C-terminal 28 PITPβ residues represent the most logical candidates for specificity elements. The rationale is threefold. First, each motif defines a region of primary sequence divergence between PITPβ and PITPα. Second, the presence of at least one element is necessary to preserve PITPβ localization to the TGN. Third, transplantation of any two motifs into PITPα efficiently redirects this protein to the TGN. Thus, the three C-terminal elements satisfy the dual criteria of necessity and sufficiency for specifying localization of a PITP reporter to TGN membranes. Whether the C-terminal specificity elements engage a proteinaceous receptor or recognize some lipid platform unique to the TGN remains an open question. However, we find PITPβ association with Golgi membranes is sensitive to brefeldin A, indicating a dependence on a functional ARF (or ARL) GTPase cycle.

We suggest the $W_{202}W_{203}$ motif contributes to PITPβ association with TGN membranes by providing a nonspecific and low-affinity membrane-binding site. Our demonstration that PITPβ association with TGN membranes is compromised by mutations of the $W_{202}W_{203}$ motif supports this view. The concept is also consistent with structural data indicating $W_{202}W_{203}$ lies on a loop oriented on the same face of the PITPβ as the mouth of the phospholipid-binding pocket (Yoder *et al.*, 2001; Tilley *et al.*, 2004). The $W_{202}W_{203}$ motif does not confer specificity of membrane binding because this element is common to both PITPα and PITPβ, and these PITPs exhibit distinct localization profiles.

Although the idea that $W_{202}W_{203}$ functions in a nonspecific and low-affinity membrane-binding reaction has its justification, other data do not readily conform to such a model. Alanine scanning mutagenesis indicates this motif has no major role in PITPβ phospholipid-transfer activity or loading with a phospholipid substrate. It could be argued this result is inconsistent with a nonspecific membrane-binding function for $W_{202}W_{203}$. We do not favor this interpretation because the phospholipid-transfer assays and yeast phenotypic rescue assay that we employ as functional tests are biased in favor of transient membrane associations. Such assays likely minimize the importance of a stabilization of membrane-binding function for $W_{202}W_{203}$.

The various phospholipid loading properties of PITPβ do not contribute in any obvious way to its association with the TGN. Of particular interest is the case of SM-binding/transfer because this property suggested an attractive mechanism for the specific homing of PITPβ to Golgi membranes. This mechanism was based on the dual arguments that PITPβ is distinguished from PITPα by its ability to load with SM and that the major site of SM synthesis in mammalian cells is the Golgi complex (Futerman *et al.*, 1990; Bankaitis, 2002). The fact that the TGN-targeting mechanism does not survey the phospholipid-bound state of PITPβ also has implications for models invoking a delivery function for PITPβ in supply of TGN membranes with PtdIns (e.g., to support TGN phosphoinositide pools). Other PITPs likely help execute such functions (Litvak *et al.*, 2005).

Our data indicate a concerted action of specific and general membrane-binding elements in the targeting of PITPβ to the TGN. We find the targeting process is not obligately coupled to PITPβ phosphorylation of residue S_{262} by conventional PKCs or at least two nonconventional PKC isoforms. That conclusion is supported by both PKCδ$^{-/-}$ and PKCε$^{-/-}$ MEF data, and the general resistance of PITPβ TGN association to challenge of cells with inhibitors of conventional PKCs. Moreover, PITPβ TGN localization signals accommodate an array of side chains at residue S_{262}—indicating neither S_{262} itself, nor its phosphorylation, is an essential component of PITPβ TGN-targeting information. The fact that combined mutagenesis to alanine of PITPβ residues S_{262} and S_{165} (a minor PKC phosphorylation site in vitro) has no effect on PITPβ localization further emphasizes this point. We expect these general findings will hold equally true for the novel PITPβ^{QGQR} spliceoform.

Our collective results are comprehensively at odds with the report of van Tiel *et al.* (2002), who claim that phosphorylation of residue S_{262} is required for Golgi membrane localization of PITPβ. Can these conflicting conclusions be reconciled? van Tiel *et al.* (2002) utilized stable NIH3T3 cell lines that overproduce PITPβ for their studies. One formal possibility is that the visible pool of PITPβ in those stable cell lines behaves differently from the endogenous pool. We do not favor this interpretation because the PITPβ-GFP chimera we used consistently localized to TGN membranes with the same fidelity as endogenous PITPβ. Also, because van Tiel *et al.* were clearly monitoring PITPβ, and not PITPβ^{QGQR}, the discrepancies cannot be ascribed to spliceoform issues. The possibility that NIH3T3 cells used by van Tiel *et al.* behave differently than MEFs or COS-7 cells cannot be formally excluded, although the absolute efficiencies of PITP-GFP targeting to the TGN in MEFs and COS-7 cells were consistently similar.

The van Tiel *et al.* (2002) report suggests several areas of experimentation that leave room for ambiguity of interpretation. First, the parameters of what constitutes a Golgi profile in their studies were not defined by the use of known

Golgi markers, and no quantification of the imaging data was presented. Second, there was no description of controls for monitoring what effect pharmacological inhibition of conventional PKCs has on Golgi organization in their cell lines. Perturbation of Golgi organization may complicate interpretation of PITPβ localization data. Third, the scope of the mutagenesis from which van Tiel *et al.* reached their conclusions was limited to a single mutant (PITPβ^{S262A}). The issue of sufficiency of S_{262} phosphorylation for PITP targeting to Golgi membranes was not addressed. Finally, the arguments that PITPβ residue S_{262} represents a major in vivo phosphorylation site are based on in vitro schemes using recombinant proteins (van Tiel *et al.*, 2002). Direct identification of phosphorylation sites in endogenous PITPβ is required to resolve this important issue.

A remarkable facet of the biological activities of PITPs is the dedication with which these proteins couple to specific physiological functions (Routt and Bankaitis, 2004; Phillips *et al.*, 2006). The example of PITPα and PITPβ is clear testimony to this effect as these closely related PITP isoforms assume radically different localization profiles and are functionally nonredundant. Our finding that murine cells can express what are likely two biochemically indistinguishable PITPβ spliceoforms, and yet localize both to similar regions of the Golgi stack, suggests that even finer functional distinctions may yet exist. Our analyses of how PITPβ targets to specific Golgi subcompartments gives us the ability to interchange, in a rational and directed way, either the localization, or the phospholipid-binding properties, or both, of PITPα and of defined PITPβ spliceoforms. This facility permits direct experimental address, in the mouse, of whether the distinct biological activities of these proteins are strictly a function of protein localization or whether differential phospholipid-binding properties also contribute to function.

ACKNOWLEDGMENTS

We thank Con Beckers and Doug Cyr for helpful discussions and insightful criticisms throughout this work, and the assistance of Michael Chua and Jan Sinyshyn of the Michael Hooker Microscopy Core (UNC) is acknowledged. Bruce Hamilton (UCSD), Hans-Peter Hauri (Basel), and George Helmkamp, Jr. generously donated antibodies for this study. Oligonucleotide primer synthesis and DNA sequence analyses were performed via the Lineberger Comprehensive Cancer Center Genome Analysis and Nucleic Acids Core facility. This work was supported by National Institutes of Health (NIH) Grants NS37723 and NS42651 awarded to V.A.B. K.E.I. was supported by a Cell and Molecular Biology Training Grant from the NIH (T32 GM08581), and R.P.H.H. was supported in part by a North Atlantic Treaty Organization Science Fellowship of the Netherlands Organization for Scientific Research (NWO).

REFERENCES

Alb, J. G., Jr., Gedvilaite, A., Cartee, R. T., Skinner, H. B., and Bankaitis, V. A. (1995). Mutant rat phosphatidylinositol/phosphatidylcholine transfer proteins specifically defective in phosphatidylinositol transfer: implications for the regulation of phosphatidylinositol transfer activity. Proc. Natl. Acad. Sci. USA *92*, 8826–8830.

Alb, J. G., Jr. *et al.* (2002). Genetic ablation of phosphatidylinositol transfer protein function in murine embryonic stem cells. Mol. Biol. Cell *13*, 739–754.

Alb, J. G., Jr., Cortese, J. D., Phillips, S. E., Albin, R. L., Nagy, T. R., Hamilton, B. A., and Bankaitis, V. A. (2003). Mice lacking phosphatidylinositol transfer protein-alpha exhibit spinocerebellar degeneration, intestinal and hepatic steatosis, and hypoglycemia. J. Biol. Chem. *278*, 33501–33518.

Bankaitis, V. A. (2002). The mammalian *trans*-Golgi network reveals a slick new recruiting tool. Science *108*, 325–328.

Bankaitis, V. A., Malehorn, D. E., Emr, S. D., and Greene, R. (1989). The *Saccharomyces cerevisiae* SEC14 gene encodes a cytosolic factor that is required for transport of secretory proteins from the yeast Golgi complex. J. Cell Biol. *108*, 1271–1281.

Bankaitis, V. A., Aitken, J. R., Cleves, A. E., and Dowhan, W. (1990). An essential role for a phospholipid transfer protein in yeast Golgi function. Nature *347*, 561–562.

Carmen-Lopez, M., Nicaud, J.-M., Skinner, H. B., Vergnolle, C., Kader, J. C., Bankaitis, V. A., and Gaillardin, C. (1994). A phosphatidylinositol/phosphatidylcholine transfer protein is required for differentiation of the dimorphic yeast *Yarrowia lipolytica* from the yeast to the mycelial form. J. Cell Biol. *124*, 113–127.

Cleves, A. E., McGee, T., and Bankaitis, V. A. (1991a). Phospholipid transfer proteins: a biological debut. Trends Cell Biol. *1*, 31–34.

Cleves, A. E., McGee, T. P., Whitters, E. A., Champion, K. M., Aitken, J. R., Dowhan, W., Goebl, M., and Bankaitis, V. A. (1991b). Mutations in the CDP-choline pathway for phospholipid biosynthesis bypass the requirement for an essential phospholipid transfer protein. Cell *64*, 789–800.

Cunningham, E., Tan, S. K., Swigart, P., Hsuan, J., Bankaitis, V. A., and Cockcroft, S. (1996). The yeast and mammalian isoforms of phosphatidylinositol transfer protein can all restore phospholipase C mediated inositol lipid signaling in cytosol-depleted RBL-2H3 and HL-60 cells. Proc. Natl. Acad. Sci. USA *93*, 6589–6593.

De Camilli, P., Emr, S. D., McPherson, P. S., and Novick, P. (1996). Phosphoinositides as regulators in membrane traffic. Science *271*, 1533–1539.

De Vries, K. J., Heinrichs, A. A., Cunningham, E., Brunink, F., Westerman, J., Somerharju, P. J., Cockcroft, S., Wirtz, K. W., and Snoek, G. T. (1995). An isoform of the phosphatidylinositol-transfer protein transfers sphingomyelin and is associated with the Golgi system. Biochem. J. *310*, 643–649.

De Vries, K. J., Westerman, J., Bastiaens, P. I., Jovin, T. M., Wirtz, K. W., and Snoek, G. T. (1996). Fluorescently labeled phosphatidylinositol transfer protein isoforms (alpha and beta), microinjected into fetal bovine heart endothelial cells, are targeted to distinct intracellular sites. Exp. Cell Res. *227*, 33–39.

Fullwood, Y., dos Santos, M., and Hsuan, J. J. (1999). Cloning and characterization of a novel human phosphatidylinositol transfer protein, rdgBβ. J. Biol. Chem. *274*, 31553–31558.

Futerman, A. H., Stieger, B., Hubbard, A.L., and Pagano, R. E. (1990). Sphingomyelin synthesis in rat liver occurs predominantly at the cis and medial cisternae of the Golgi apparatus. J. Biol. Chem. *25*, 8650–8657.

Hay, J. C., and Martin, T.F.J. (1993). Phosphatidylinositol transfer protein is required for ATP-dependent priming of Ca^{2+}-activated secretion. Nature *366*, 572–575.

Ito, H., Fukuda, Y., Murata, K., and Kimura, A. (1983). Transformation of intact yeast cells treated with alkaline cations. J. Bacteriol. *153*, 163–168.

Jones, S. M., Alb, J. G., Jr., Phillips, S. E., Bankaitis, V. A., and Howell, K. E. (1998). A phosphatidylinositol 3-kinase and phosphatidylinositol transfer protein act synergistically in formation of constitutive transport vesicles from the trans-Golgi network. J. Biol. Chem. *273*, 10349–10354.

Kearns, B. G., McGee, T. P., Mayinger, P., Gedvilaite, A., Phillips, S. E., Kagiwada, S., and Bankaitis, V. A. (1997). An essential role for diacylglycerol in protein transport from the yeast Golgi complex. Nature *387*, 101–105.

Kearns, M. A., Monks, D. E., Fang, M., Rivas, M. P., Courtney, P. D., Chen, J., Prestwich, G. D., Theibert, A. B., Dewey, R. E., and Bankaitis, V. A. (1998). Novel developmentally regulated phosphoinositide binding proteins from soybean whose expression bypasses the requirement for an essential phos phatidylinositol transfer protein in yeast. EMBO J. *17*, 4004–4017.

Lehel, C., Olah, Z., Jakab, G., and Anderson, W. B. (1995). PKC epsilon is localized to the Golgi via its zinc-finger domain and modulates Golgi function. Proc. Natl. Acad. Sci. USA *92*, 1406–1410.

Li, X., Routt, S., Xie, Z., Cui, X., Fang, M., Kearns, M. A., Bard, M., Kirsch, D., and Bankaitis, V. A. (2000). Identification of a novel family of nonclassical yeast PITPs whose function modulates activation of phospholipase D and Sec14p-independent cell growth. Mol. Biol. Cell *11*, 1989–2005.

Litvak, V., Dahan, N., Ramachandran, S., Sabanay, H., and Lev, S. (2005). Maintenance of the diacylglycerol level in the Golgi apparatus by the Nir2 protein is critical for Golgi secretory function. Nat. Cell Biol. *7*, 225–234.

Nakase, Y., Nakamura, T., Hirata, A., Routt, S. M., Skinner, H. B., Bankaitis, V. A., and Shimoda, C. (2001). The *Schizosaccharomyces pombe* spo20(+) gene encoding a homologue of *Saccharomyces cerevisiae* Sec14 plays an important role in forespore membrane formation. Mol. Biol. Cell *4*, 901–917.

Ohashi, M., de Vries, K. J., Frank, R., Snoek, G., Bankaitis, V. A., Wirtz, K., and Huttner, W. B. (1995). A role for phosphatidylinositol transfer protein in secretory vesicle formation. Nature *377*, 544–547.

Phillips, S. E., Vincent, P., Rizzieri, K., Schaaf, G., Gaucher, E. A., and Bankaitis, V. A. (2006). The diverse biological functions of phosphatidylinositol transfer proteins in eukaryotes. Crit. Rev. Biochem. Mol. Biol. *41*, 21–49.

Phillips, S. E. *et al.* (1999). Yeast Sec14p deficient in phosphatidylinositol transfer activity is functional in vivo. Mol. Cell *4*, 187–197.

Routt, S. M., and Bankaitis, V. A. (2004). Biological functions of phosphatidylinositol transfer proteins. Biochem. Cell Biol. *82*, 254–262.

Schouten, A., Agianian, B., Westerman, J., Kroon, J., Wirtz, K. W., and Gros, P. (2002). Structure of apo-phosphatidylinositol transfer protein alpha provides insight into membrane association. EMBO J. *21*, 2117–2121.

Sha, B. D., Phillips, S. E., Bankaitis, V. A., and Luo, M. (1998). Crystal structure of the *Saccharomyces cerevisiae* phosphatidylinositol transfer protein. Nature *391*, 506–510.

Sherman, F., Fink, G. R., and Hicks, J. B. (1983). Methods in Yeast Genetics, Cold Spring Harbor, NY: Cold Spring Harbor Laboratory Press.

Simonsen, A., Wurmser, A. E., Emr, S. D., and Stenmark, H. (2001). The role of phosphoinositides in membrane transport. Curr. Opin. Cell Biol. *13*, 485–492.

Skinner, H. B., Alb, Jr., J. G., Whitters, E. M., Helmkamp, G. M., Jr., and Bankaitis, V. A. (1993). Phospholipid transfer activity is relevant to but not sufficient for the essential function of the yeast SEC14 gene product. EMBO J. *12*, 4775–4784.

Storz, P., Döppler, H., and Toker, A. (2004). PKCδ selectively regulates protein kinase D-dependent activation of NF-κB in oxidative stress signaling. Mol. Cell. Biol. *24*, 2614–2626.

Tanaka, S., and Hosaka, K. (1994). Cloning of a cDNA encoding a second phosphatidylinositol transfer protein from rat brain by complementation of the yeast sec14 mutation. J. Biochem. *115*, 981–984.

Tilley, S. J., Skippen, A., Murray-Rust, J., Swigart, P. M., Stewart, A., Morgan, C. P., Cockcroft, S., and McDonald, N. Q. (2004). Structure-function analysis of phosphatidylinositol transfer protein alpha bound to human phosphatidylinositol. Structure *12*, 317–326.

van Tiel, C. M., Westerman, J., Paasman, M., Wirtz, K. W., and Snoek, G. T. (2000). The PKC-dependent phosphorylation of serine 166 is controlled by the phospholipid species bound to the phosphatidylinositol transfer protein alpha. J. Biol. Chem. *275*, 21532–21538.

van Tiel, C. M., Westerman, J., Paasman, M., Hoebens, M. M., Wirtz, K. W., and Snoek, G. T. (2002). The Golgi localization of phosphatidylinositol transfer protein β requires the PKC-dependent phosphorylation of serine 262 and is essential for maintaining plasma membrane sphingomyelin levels. J. Biol. Chem. *277*, 22447–22452.

Vincent, P., Chua, M. Nogue, F., Fairbrother, A., Mekheel, H., Xu, Y., Allen, N., Bibikova, T. N., Gilroy, S., and Bankaitis, V. A. (2005). A Sec14p-nodulin domain phosphatidylinositol transfer protein polarizes membrane growth of *Arabidopsis thaliana* root hairs. J. Cell Biol. *168*, 801–812.

Yoder, M. D., Thomas, L. M., Tremblay, J. M., Oliver, R. L., Yarbrough, L. R., and Helmkamp, M., Jr. (2001). Structure of a multifunctional protein. Mammalian phosphatidylinositol transfer protein complexed with phosphatidylcholine. J. Biol. Chem. *276*, 9246–9252.